Available online at www.sciencedirect.com
ScienceDirect
Deep-Sea Research II 54 (2007) 1469–1485
DEEP-SEA RESEARCH PART II
www.elsevier.com/locate/dsr2

Depth distributions of alkalinity, TCO_2 and $\delta^{13}C_{TCO_2}$ at SEATS time-series site in the northern South China Sea

W.C. Chou[a,b], D.D. Sheu[c,*], B.S. Lee[d], C.M. Tseng[a,e], C.T.A. Chen[c], S.L. Wang[f], G.T.F. Wong[g]

[a]*National Center for Ocean Research, P.O. Box 23-13, Taipei 106, Taiwan, ROC*
[b]*Institute of Marine Environmental Chemistry and Ecology, National Taiwan Ocean University, 2, Pei-Ning Rd., Keelung, Taiwan, ROC*
[c]*Institute of Marine Geology and Chemistry, National Sun Yat-Sen University, Kaohsiung 804, Taiwan, ROC*
[d]*Department of Biotechnology, ChungChou Institute of Technology, Yuanlin, Changhua 510, Taiwan, ROC*
[e]*Institute of Oceanography, National Taiwan University, P.O. Box 23-13, 106 Taipei , Taiwan, ROC*
[f]*Department of Marine Environmental Engineering, National Kaohsiung Marine University, Kaohsiung, Taiwan, ROC*
[g]*Research Center for Environmental Changes, Academia Sinica, 128, Academia Road, Section 2, Nankang, 115 Taipei, Taiwan, ROC*

Accepted 10 May 2007
Available online 10 July 2007

Abstract

In this study, measurements of titration alkalinity (TA), total dissolved carbon dioxide (TCO_2), and $\delta^{13}C$ of TCO_2 ($\delta^{13}C_{TCO_2}$) throughout the water column at the SouthEast Asian time-series study (SEATS) site were investigated in order to understand better the fundamental processes controlling their vertical distributions in the South China Sea (SCS). The linear correlations between TA and salinity in the shallow waters, as identified by the mixing line between the surface water and salinity maximum water suggested the predominant control of physical mixing on the variability of TA. In contrast, TCO_2 and $\delta^{13}C_{TCO_2}$ showed the non-conservative behavior in the respective TCO_2 and $\delta^{13}C_{TCO_2}$ vs. salinity plot due to the effect of biological production. A stoichiometric model further showed that the depth profile of NTA (= TA × salinity/35) largely reflects the increase of preformed NTA in the shallow waters, whereas carbonate dissolution was responsible for the continuous increase of NTA in the deep waters. A one-dimensional diffusion–advection model further revealed that the carbonate dissolution could account for 28% of $NTCO_2$ (= TCO_2 × salinity/35) increase in deep waters, and the remaining 72% of $NTCO_2$ was from organic decomposition. Calculation of excess TA further showed that it emerged well above the aragonite and calcite saturation depths at 600 and 2500 m, respectively, indicating that some biologically, chemically, and physically-mediated processes must be involved to provide excess TA into the shallow waters. The decrease in $\delta^{13}C_{TCO_2}$ with depth primarily resulted from organic decomposition.

The influence of anthropogenic CO_2 throughout the water column was assessed with the carbon chemistry and the isotope-based approach in this study. Both methods obtained nearly the same results in which the signal of anthropogenic CO_2 decreased exponentially with depth, and its penetration depth were found to be at ~1000 m. The inventory of anthropogenic CO_2 in the water column was estimated to be ~16.6 mol C m^{-2}, which was less than that reported in the northwest Pacific at the same latitude, presumably due to the enhanced upwelling in the SCS. Such an anthropogenic CO_2

*Corresponding author. Tel.: +886 7 525 5148; fax: +886 7 525 5348.
E-mail address: ddsheu@mail.nsysu.edu.tw (D.D. Sheu).

0967-0645/$ - see front matter
doi:10.1016/j.dsr2.2007.05.002

penetration had led to decreases of the saturation levels of aragonite and calcite by 17% and 14%, respectively, in the surface water, and an upward migration of aragonite saturation depth by ~100 m since industrial revolution.

Keywords: Anthropogenic CO_2; Carbon chemistry; South China Sea

1. Introduction

Recent concerns about the role of ocean in regulating the atmospheric CO_2 concentration have prompted oceanographers to reexamine the fundamental processes controlling the distributions of total dissolved carbon dioxide (TCO_2), total alkalinity (TA), and $\delta^{13}C$ of TCO_2 ($\delta^{13}C_{TCO_2}$) in seawater, because these parameters not only provide insight into our current understanding of anthropogenic CO_2 in the oceans, e.g., the penetration and storage of anthropogenic CO_2, but also can be used as a baseline for future estimates of oceanic CO_2 uptake (Wallace, 2001; Quay et al., 2003). For instance, results from the WOCE/JGOFS program and other studies in 1990s have greatly improved our knowledge of the fate of anthropogenic CO_2 and its impact on carbonate system in the oceans (Sabine et al., 2004; Feely et al., 2004 and references therein). Nonetheless, most of these studies were conducted in open-ocean regimes with very limited data available in the marginal seas, despite the fact that ~20% of the global ocean's net annual uptake of anthropogenic CO_2 ($0.4\,Pg\,C\,yr^{-1}$) may have been sequestrated in the marginal seas and delivered to the open ocean via the "continental shelf pump" (Thomas et al., 2004).

In order to better understand the role of marginal seas in marine carbon cycles, a time-series program (i.e. the SouthEast Asian time-series study, SEATS) was initiated in 1998 in the northern South China Sea (SCS; Fig. 1). The seasonal variability of carbon parameters within the mixed layer at SEATS was reported previously by Chou et al. (2005, 2006) and a long-term variation trend can be found in Tseng et al. (2007). Here, instead of discussing their temporal variations, we have compiled the high quality data collected from 19 cruises at the SEATS site to examine the general processes controlling the vertical variations of NTA (normalized TA = TA × 35/salinity), $NTCO_2$ (normalized $TCO_2 = TCO_2 \times 35$/salinity) and $\delta^{13}C_{TCO_2}$ below the surface mixed layer, and to evaluate the influences of anthropogenic CO_2 in the water column. The techniques employed in this study to examine the carbon system and the influence of anthropogenic CO_2 are similar to those applied in the North Pacific so that results from SEATS can be compared to the results from its major source area, i.e. the North Pacific. Moreover, results from this study also shed light on our current understanding of the role of SCS in the uptake of anthropogenic CO_2, and could be used as a baseline for future evaluation of the long-term variability of the carbon system in the SCS. However, it is worth to note that since our data are limited to a single site, potential influences of horizontal processes on the vertical characters delineated in this study are largely ignored.

2. Methods

During the course of this study, the SEATS site was investigated 19 times from September 1999 to October 2003 aboard *R/V Ocean Research I* or *III* (September and November 1999, January, March, May, July, and October 2000, February, June, October, and December 2001, March, July, September, and November 2002, as well as January, March, August and October 2003). All raw data of TA and TCO_2 and other pertinent measurements of SEATS are archived in the Ocean Data Bank (ODB) at the National Center for Ocean Research. Interested readers may contact NCOR-ODB for data requests (NCOR; http://www.ncor.ntu.edu.tw/ODBS/). Discrete water samples for TCO_2, TA and $\delta^{13}C_{TCO_2}$ analyses were transferred into 250 ml BOD bottles from Go-Flo bottles mounted onto a Rosette sampling assembly. All water samples were poisoned with 200 μl saturated $HgCl_2$ solution immediately after collection and stored at 5 °C in darkness to prevent biological alteration.

TCO_2 and TA were determined following the standard operating procedures described in DOE (1994). The coulometric method was used for TCO_2 measurements with a precision of 0.1%. The single operator multiparameter metabolic analyzer (SOMMA) system was used to extract CO_2 from acidified seawater samples, and the extracted CO_2 was quantified by a coulometric detector (UIC, coulometric Inc., model 5011). TA was determined by the

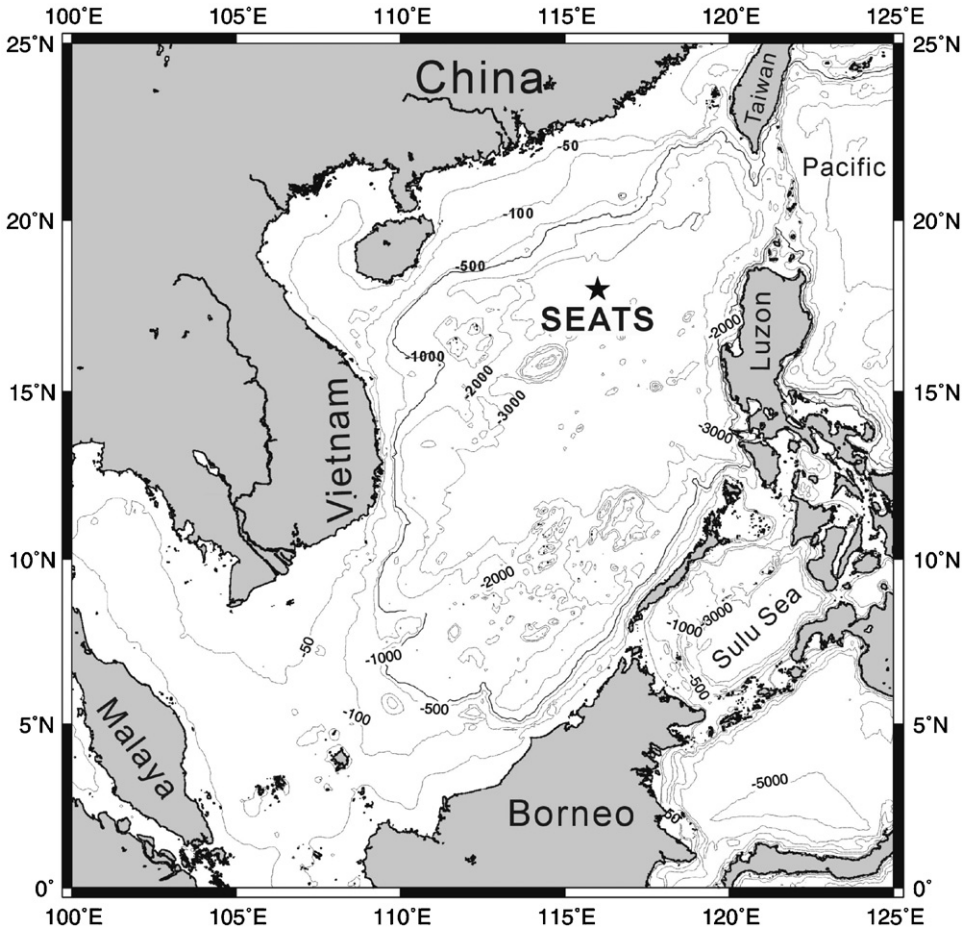

Fig. 1. Bathymetric map showing the location of the South East Asian time-series study (SEATS) site (18°15′N, 115°35′E). Contours are in meters.

potentiometric titration method with a precision of 0.2%. The titration data passing the carbonic acid endpoint (~4.5 pH) were calculated to obtain TA using the mass and charge balance method developed by Butler (1992). Seawater references prepared and provided by A.G. Dickson were used throughout this study for calibration and accuracy assessment. The differences between the certified values and our measurements were less than 2 and 3 μmol kg^{-1} for TCO_2 and TA, respectively.

For $\delta^{13}C_{TCO_2}$ analysis, 40 ml of sample were injected into a pre-evacuated vessel and then reacted with 2 ml 85% H_3PO_4 to liberate TCO_2. The evolved CO_2 was trapped in a 6-mm glass finger submerged in liquid nitrogen after complete removal of water vapor and other condensable gases by a slurry of dry ice and alcohol mixture, and then torch sealed (Sheu et al., 1996). Isotopic analysis was performed with a VG Optima mass spectrometer. Results of isotopic measurement were expressed with the conventional δ notation and reported as per mil (‰) difference relative to the PDB standard (Craig, 1957). The overall procedural error for $\delta^{13}C_{TCO_2}$ analyses was better than ± 0.05‰. It should be noted that, unlike TCO_2 and TA analyses, which began on September 1999, $\delta^{13}C$ analysis was performed on samples collected after March 2002.

The analytical uncertainties in TCO_2, TA and $\delta^{13}C_{TCO_2}$ were further verified by their variations in deep waters (>2000 m), where they should remain constant through time. The variations ($\pm 1\sigma$) of TCO_2, TA and $\delta^{13}C_{TCO_2}$ at σ_t of 27.63 ± 0.01 (corresponding to the depth of 2500 ± 200 m) were 1.9, 2.4 μmol kg^{-1}, and 0.03‰, respectively (Fig. 2). These variations are all less than the reported analytical errors, and thus lend to the credit of the high quality of our data.

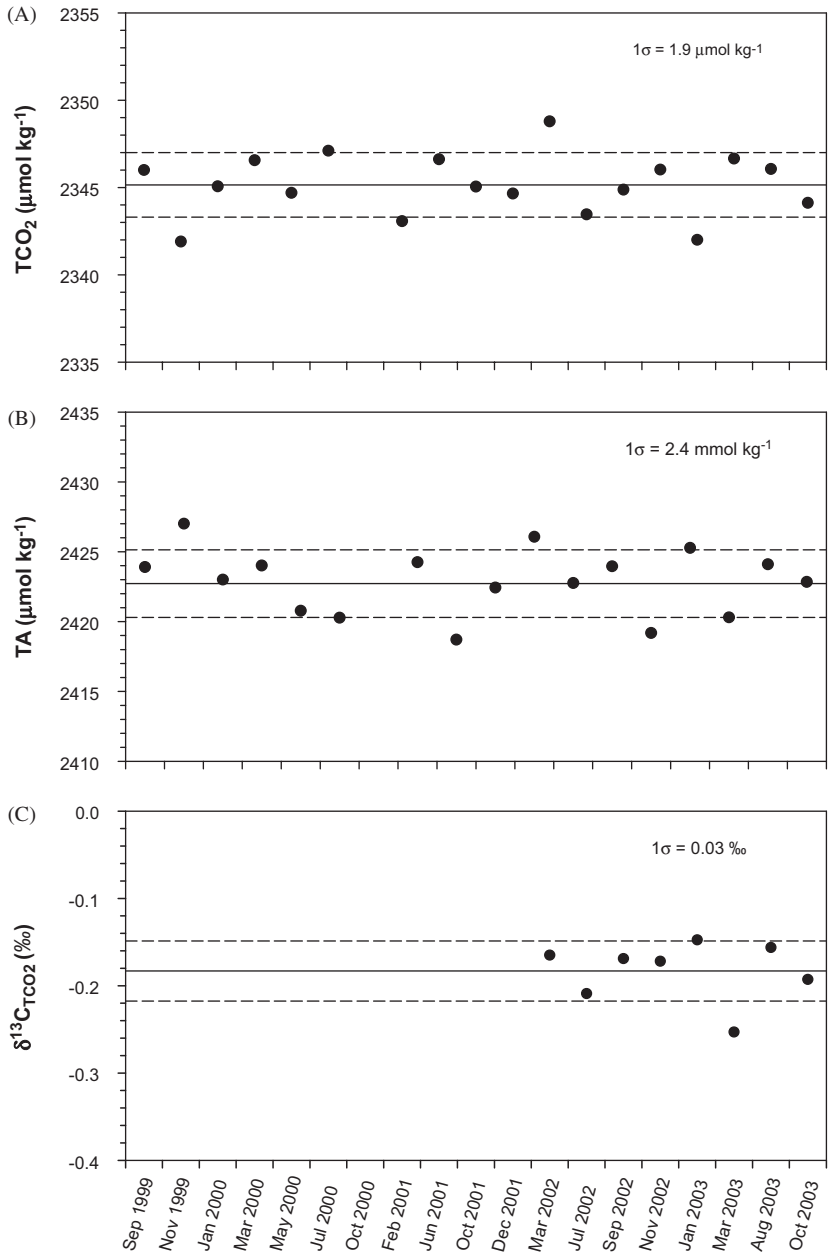

Fig. 2. Variations of (A) TCO_2 (B) TA, and (C) $\delta^{13}C_{TCO_2}$ at σ_t of 27.63 ± 0.01 (corresponding to the depth of 2500 ± 200 m) from the 19 cruises between September 1999 and October 2003 at the SEATS site. Note the measurements of $\delta^{13}C_{TCO_2}$ started from March 2002.

3. Results and discussion

3.1. Water mass structure and its role on the vertical distributions of TA, TCO_2, and $\delta^{13}C_{TCO_2}$

Since the northwestern Pacific (NWP) is the primary source of open-ocean water to the SCS, the SCS shares an analogous water mass structure with NWP, i.e. both are characterized by extremes in salinity (Gong et al., 1992). The plot of potential temperature vs. salinity (Fig. 3) at SEATS clearly shows linear trends that can be inferred to be the result of mixing of the four distinct water masses, namely the surface water (SW), salinity maximum water ($S_{max}W$), salinity minimum water ($S_{min}W$), and deep water (DW). The low salinity of SW is due to basin-wide precipitation and river runoff from the surrounding landmass. The $S_{max}W$ with a

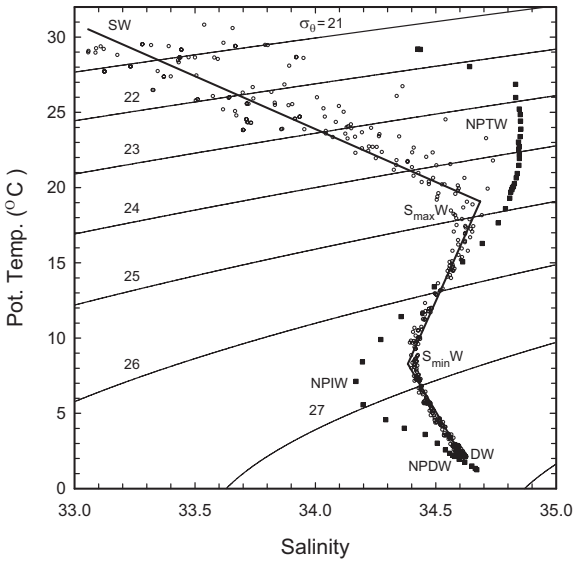

Fig. 3. Potential temperature vs. salinity relationships at the SEATS site (open circles) and adjacent northwestern Pacific (solid squares). SW, $S_{max}W$, $S_{min}W$, and DW indicate the surface water, salinity maximum water, salinity minimum water, and deep water, respectively, in the South China Sea (SCS). NPTW, NPIW, and NPDW denote North Pacific tropical water, North Pacific intermediate water, and North Pacific deep water, respectively. Solid lines represent the hypothetically linear mixing lines between the four water masses in the SCS.

salinity of ~34.65 centered at approximate 150 m is indicative of the North Pacific tropical water (Nitani, 1972). The core of $S_{min}W$ with a salinity of ~34.40 at about 500 m fingerprints the North Pacific intermediate water (Nitani, 1972). Nonetheless, it is worth to note that due to the intensive upwelling and vertical mixing, the salinity extremes in the SCS become less pronounced than those in NWP (Shaw et al., 1996), i.e. salinity maximum becomes smaller (~34.6 vs. ~34.9) but salinity minimum becomes larger (~34.4 vs. ~34.2) in the SCS (Fig. 3). The DW bears nearly the same properties as the water from the adjacent NWP through the Luzon Strait at a sill depth of ~2200 m, indicating that DW in the SCS originates mainly from the North Pacific deep water (NPDW; Gong et al., 1992; Chen et al., 2006).

Fig. 4 depicts the distributions of TA, TCO_2, and $\delta^{13}C_{TCO_2}$ vs. salinity at the SEATS site. As shown in Fig. 4A, the relationships between TA and salinity fit well with the linear mixing lines in the shallow waters (waters between SW and $S_{max}W$; line A in Fig. 4A), evidencing that the physical mixing rates are faster than TA changes caused by biological processes. On the contrary, TCO_2 and $\delta^{13}C_{TCO_2}$ vs. salinity plots show a nonlinear mixing in the shallow waters, suggesting that biological production of carbonate and organic carbon is predominant in defining the depth distributions of TCO_2 and $\delta^{13}C_{TCO_2}$ in the shallow waters, and consequently results in the observed lower TCO_2 and heavier $\delta^{13}C_{TCO_2}$ with respect to their hypothetical linear mixing line (line A in Fig. 4B and C).

By comparison, TA, TCO_2 and $\delta^{13}C_{TCO_2}$ vs. salinity plots all show nonlinear mixing in the deep waters (waters between $S_{min}W$ and DW), where TA, TCO_2 are higher and $\delta^{13}C_{TCO_2}$ is lighter than their theoretical values expected from the purely linear mixing lines (line C in Fig. 4A–C). This non-linearity indicates that organic matter decomposition and carbonate dissolution are the responsible processes for the vertical distributions of TA, TCO_2 and $\delta^{13}C_{TCO_2}$ observed in the deep waters. Moreover, TA, TCO_2 and $\delta^{13}C_{TCO_2}$ vs. salinity plots also demonstrate a nonlinear mixing trend in the intermediate waters (waters between $S_{max}W$ and $S_{min}W$). Nonetheless, this non-linearity hardly results from the non-conservative biological production, because the depth range of intermediate waters (~150–~500 m) is far below the euphotic zone (80–90 m) where major biological production is taking place. Therefore, the physical mixing among three end members, i.e. SW, $S_{max}W$, $S_{min}W$, is more likely responsible for the observed non-linearity with lower TA and TCO_2 and heavier $\delta^{13}C_{TCO_2}$.

3.2. *Analyses of controlling factors on the depth variations of NTA, $NTCO_2$ and $\delta^{13}C_{TCO_2}$ in the water column at the SEATS site*

It has been well recognized that TA, TCO_2, and $\delta^{13}C_{TCO_2}$ measured in the water column consist of three major components: (1) the preformed values, i.e. values of a water mass at the time of its formation at surface outcrops; (2) changes resulting from organic decomposition (the organic carbon pump); (3) changes caused by the carbonate dissolution (the carbonate pump). Accordingly, their measured values at any given depth in the water column can be represented respectively by the following equations (Chen and Millero, 1979; Kroopnick, 1985; Feely et al., 2002):

$$NTA^{meas} = NTA^{pre} + TA^{org} + TA^{carb}, \quad (1)$$

$$NTCO_2^{meas} = NTCO_2^{pre} + TCO_2^{org} + TCO_2^{carb}, \quad (2)$$

$$\delta^{13}C^{meas} = \delta^{13}C^{pre} + \delta^{13}C^{org} + \delta^{13}C^{carb}, \quad (3)$$

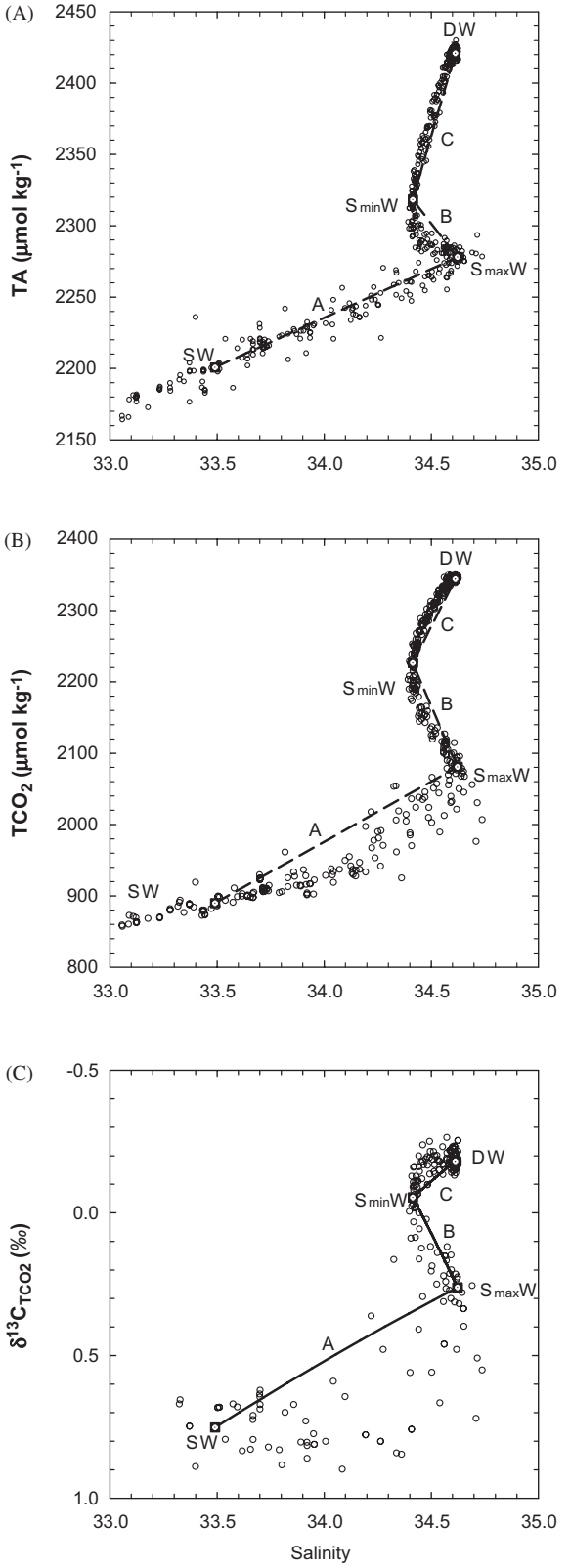

where the superscripts "meas", "pre", "org" and "carb" stand for measured, preformed, organic decomposition and carbonate dissolution, respectively. In Eqs. (1) and (2), TA and TCO_2 were normalized to a constant salinity of 35 (NTA and $NTCO_2$) to remove the effect of evaporation/precipitation on their variations. In the following discussion, we will apply these equations to assess their relative contribution to the observed depth variations of NTA, $NTCO_2$, and $\delta^{13}C_{TCO_2}$ at the SEATS site. Data from all 19 cruises were averaged to carry out these assessments.

3.2.1. NTA

The preformed TA equation of Sabine et al. (2002a) was used to calculate the TA^{pre} values,

$$TA^{pre} = 148.7 + (61.36 \times S) + (0.0941 \times PO) - (0.582 \times \theta), \quad (4)$$

where S is salinity, PO is a quasi-conservative tracer (PO = dissolved oxygen + 170 × phosphate), and θ is the potential temperature. The reason for choosing this equation lies in the fact that it was derived from the WOCE/JGOFS data in the surface water (0–60 m) of entire Pacific and, as mentioned earlier, that the SCS water originates mainly from the NWP. Results (Fig. 5, open squares) show that NTA^{pre} increases gradually from surface to approximately 1500 m, and then remains essentially constant below 1500 m. The increase in NTA^{pre} with depth therefore accounts for, in part, the observed vertical gradient of NTA^{meas} in the water column, especially in the shallow waters.

The component "TA^{org}" in Eq. (1) represents the change of TA due to production and/or remineralization of organic matters. Conventionally, the net effect between organic production and decomposition on TA changes is estimated by apparent oxygen utilization (AOU). In this study, we adopted a coefficient of 0.119 of Feely et al. (2002) to calculate

Fig. 4. (A) TA, (B) TCO_2, and (C) $\delta^{13}C_{TCO_2}$ vs. salinity relationships at the SEATS site. SW, $S_{max}W$, $S_{min}W$, and DW denote the surface water, salinity maximum water, salinity minimum water, and deep water, respectively, in the South China Sea. Dashed lines in (A) and (B) represent the hypothetically linear mixing lines between the four water masses. Solid lines in (C) represent the hypothetically non-linear mixing lines for $\delta^{13}C_{TCO_2}$ between the four water masses. The end members of SW, $S_{max}W$, $S_{min}W$, and DW were determined as the averages of all data collected in top 10 m, at the depth of 150, 500 m, and greater than 2500 m, respectively, from the 19 cruises between September 1999 and October 2003.

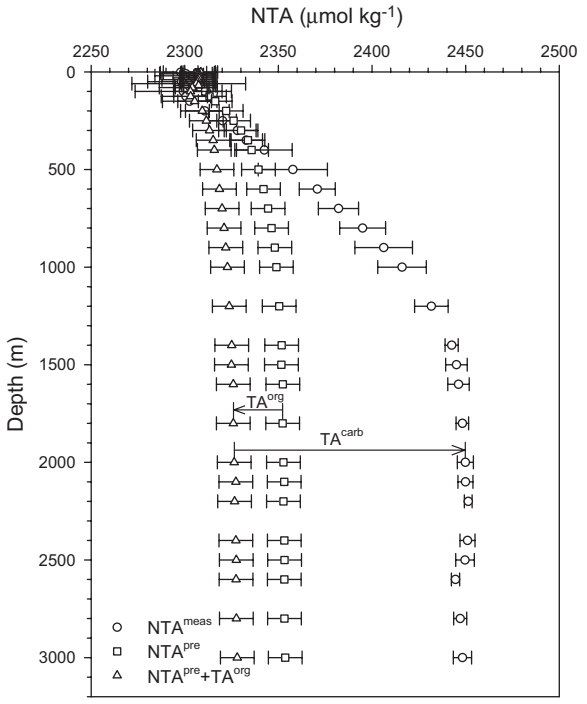

Fig. 5. Depth profiles of measured NTA (NTA^{meas}), preformed NTA (NTA^{pre}), and $NTA^{pre}+TA^{org}$ at the SEATS site. See details in text for the definitions and calculations of TA^{org} and TA^{carb}. Open circle and horizontal bar represent the average and variation of NTA^{meas} at a given depth from the 19 cruises between September 1999 and October 2003. Horizontal bars on NTA^{pre} and $NTA^{pre}+TA^{org}$ profiles represent the uncertainties in their calculations.

the TA^{org},

$$TA^{org} = -0.119 \times AOU. \quad (5)$$

The above conversion includes the contributions from nitrate, organic phosphorus and sulfur, and assumes a nitrate/AOU ratio of 16/170 (Anderson and Sarmiento, 1994). The magnitude of TA^{org} is graphically represented by the difference between NTA^{pre} (open squares) and ($NTA^{pre}+TA^{org}$) (open triangles) in Fig. 5.

The amount of TA produced by carbonate dissolution (TA^{carb}) can be readily computed by subtracting ($NTA^{pre}+TA^{org}$) from NTA^{meas}, as formulated in Eq. (1). As shown, TA^{carb} (the difference between open circles and triangles) appears below 200 m and increases sharply to 1500 m, then remains constant to the bottom. Together, these profiles demonstrate the importance of TA^{carb} in controlling the observed large increase of NTA^{meas} in the deeper waters, whereas increase of NTA^{meas} in the shallower waters results mainly from the increase of NTA^{pre}, and TA^{org} plays a role in modulating the vertical gradient of NTA^{meas}.

3.2.2. $NTCO_2$

Referring to Eq. (2), "$NTCO_2^{meas}$" is the sum of "$NTCO_2^{pre}$", "TCO_2^{org}", and "TCO_2^{carb}", in which "TCO_2^{org}" can be evaluated from the AOU on the basis of the stoichiometric ratio (C/AOU) of 117/170 (Anderson and Sarmiento, 1994):

$$TCO_2^{org} = 117/170 \times AOU. \quad (6)$$

For "TCO_2^{carb}", it is calculated from TA^{carb} because of the fact that dissolution of $CaCO_3$ can result in an increase of TA and TCO_2 at a ratio of 2/1 (i.e. $TCO_2^{carb} = 0.5 \times TA^{carb}$). Substituting Eq. (1) and (5) into this relationship, and rearranging the equation, the term "TCO_2^{carb}" was computed as follows:

$$\begin{aligned} TCO_2^{carb} &= 0.5 \times TA^{carb} = 0.5 \\ &\quad \times (NTA^{meas} - NTA^{pre} - TA^{org}) \\ &= 0.5 \times (NTA^{meas} - NTA^{pre}) \\ &\quad + 0.0593 \times AOU. \end{aligned} \quad (7)$$

Finally, $NTCO_2^{pre}$ was calculated by subtracting ($TCO_2^{org}+TCO_2^{carb}$) from $NTCO_2^{meas}$ (ref. Eq. (2)). Results from these calculations were depicted graphically in Fig. 6. As seen, $NTCO_2^{pre}$, TCO_2^{org} (the difference between open triangles and squares), and TCO_2^{carb} (the difference between open circles and triangles) all increase gradually with depth. In terms of their relative contributions, the vertical increment of $NTCO_2^{meas}$ in the upper 400 m comes equally from the increase of $NTCO_2^{pre}$ and TCO_2^{org}. Below 400 m, although TCO_2^{carb}, $NTCO_2^{pre}$ and TCO_2^{org} all account for the continuous increase of $NTCO_2^{meas}$ with depth, TCO_2^{carb} is much less important than the other two.

The relative contribution of carbonate and organic pumps to TCO_2 increase with depth was further examined with TCO_2^{carb}/TCO_2^{org} (IC/OC) ratios. As shown in Fig. 7, IC/OC ratio increases from ~0.04 at 300 m to ~0.36 at 2000 m, and then remains fairly constant below 2000 m. The value of 0.36 indicates that approximately 26% of TCO_2 production in waters deeper than 2000 m at the SEATS site is from carbonate dissolution. This percentage of carbonate dissolution is consistent with that reported previously by Chen (1990) in the Pacific and the SCS (Table 1). The high IC/OC ratio of ~0.36 found in the deep waters of SCS also reflects its origin from the oldest and hence most corrosive water mass, i.e. NPDW. The increasing IC/OC with depth further confirms the increasing

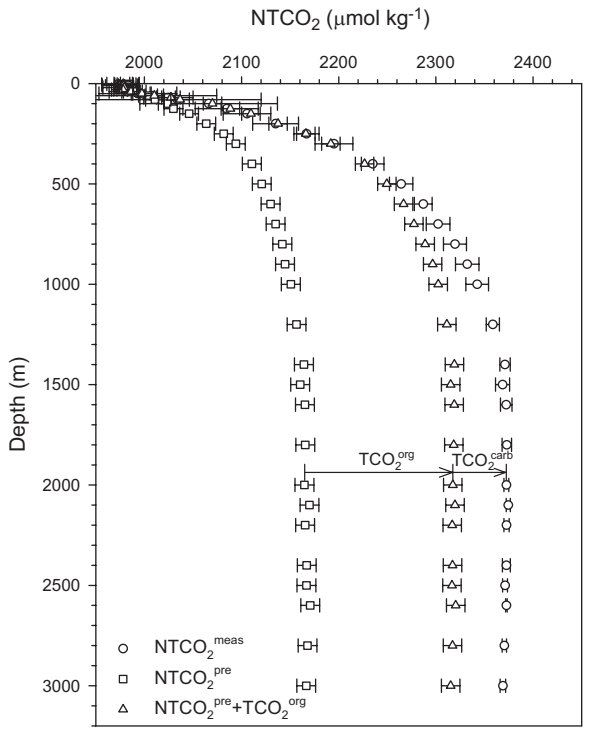

Fig. 6. Depth profiles of measured $NTCO_2$ ($NTCO_2^{meas}$), preformed $NTCO_2$ ($NTCO_2^{pre}$), and $NTCO_2^{pre}+TCO_2^{org}$ at the SEATS site. See text for the definitions and calculations of TCO_2^{org} and TCO_2^{carb} in details. Open circle and horizontal bar represent the average and variation of $NTCO_2^{meas}$ at a given depth from the 19 cruises between September 1999 and October 2003. Horizontal bars on $NTCO_2^{pre}$ and $NTCO_2^{pre}+TCO_2^{org}$ profiles represent the uncertainties in their calculations.

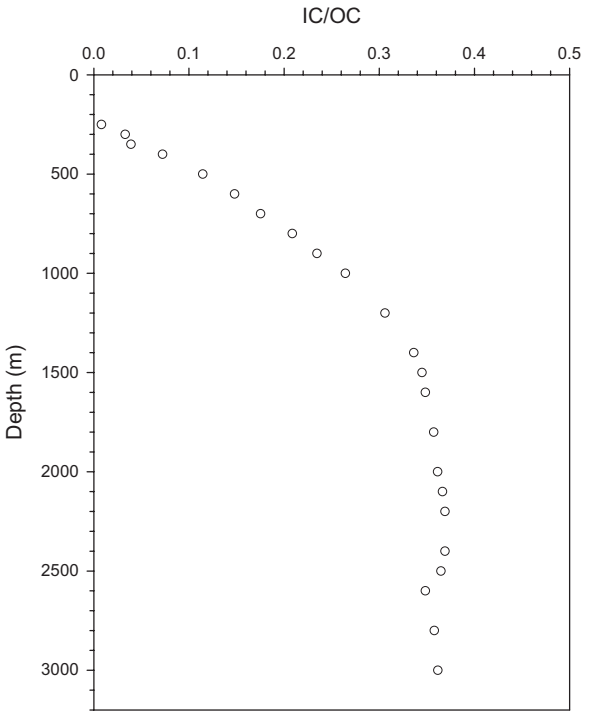

Fig. 7. Depth profiles of IC/OC ratio at the SEATS site, which implies the relative contribution of carbonate dissolution and organic decomposition to the increase of TCO_2 in water samples.

importance of carbonate dissolution with depth in water column.

Since the θ vs. salinity plot is relatively linear between the $S_{min}W$ and DW at the SEATS site, a one-dimensional advection–diffusion model can be applied to cross-check the IC/OC ratios derived from the above stoichiometric model. By taking the same technique of Craig (1969), the resultant $Z^*(=K/w)$, J/w for TA, and TCO_2 are 0.44 km, 3.60 and 6.58 μmol kg^{-1} km^{-1} (Fig. 8), respectively, where Z^*, K, w, and J represent the mixing parameter, eddy-diffusion coefficient, upwelling rate, and production rates, respectively. The calculated Z^* at SEATS is apparently lower than those reported previously in the North Pacific (0.44 vs. 0.86–1.20 km; Craig and Weiss, 1970; Chung and Craig, 1973; Table 1). Since K is relatively invariable in the ocean, the smaller Z^* at SEATS suggests a higher upwelling rate (larger w) in the SCS, which agrees well with the consensus that the rates of vertical mixing and upwelling in the SCS are high (Chao et al., 1996). Substituting the calculated values of J/w for TA ($(J/w)_{Alk}$) and TCO_2 ($(J/w)_{TCO_2}$) into the following equation:

$$IC/OC = 0.5(J/w)_{Alk}/[(J/w)_{TCO_2} - 0.5(J/w)_{Alk}], \quad (8)$$

where an IC/OC ratio of 0.38 was obtained, which agrees well with that (0.36) estimated from the stoichiometric model discussed above. This agreement further supports the validity of preformed equation used in the stoichiometric model for IC/OC estimates.

3.2.3. $\delta^{13}C_{TCO_2}$

To evaluate the respective contribution of $\delta^{13}C^{pre}$, $\delta^{13}C^{org}$ and $\delta^{13}C^{carb}$ to the observed vertical gradient of $\delta^{13}C^{meas}$, we rewrote the Eq. (3) in a mass-balance form:

$$\delta^{13}C^{meas} \times TCO_2^{meas} = \delta^{13}C^{pre} \times TCO_2^{pre} + \delta^{13}C^{org'} \times TCO_2^{org} + \delta^{13}C^{carb'} \times TCO_2^{carb}, \quad (9)$$

Table 1
Comparisons of IC/OC, Z^*, saturation depth of aragonite, saturation depth of calcite, penetration depth of anthropogenic CO_2, total column inventory of anthropogenic CO_2, $\Delta\delta^{13}C/\Delta TCO_2$ at the SEATS site with those in the North Pacific

	SEATS	North Pacific	References
IC/OC	0.36–0.38	0.36	Chen (1990)
Z^*	0.44 km	0.86–1.20 km	Craig and Weiss (1970) Chung and Craig (1973)
Saturation depth of aragonite	600m	~600 m	Feely et al. (2002)
Saturation depth of calcite	2500m	~2500 m	Feely et al. (2002)
Penetration depth of anthropogenic CO_2	~1000 m	~1000 m	Sabine et al. (2002a) Chen (1987)
Total column inventory of anthropogenic CO_2	~16.6 mol m^{-2}	~20 mol m^{-2}	Sabine et al. (2002a)
$\Delta\delta^{13}C/\Delta TCO_2$	−0.026‰ (μmol kg^{-1})$^{-1}$	−0.024‰ (μmol kg^{-1})$^{-1}$	Winn et al. (1998) Gruber et al. (1999)

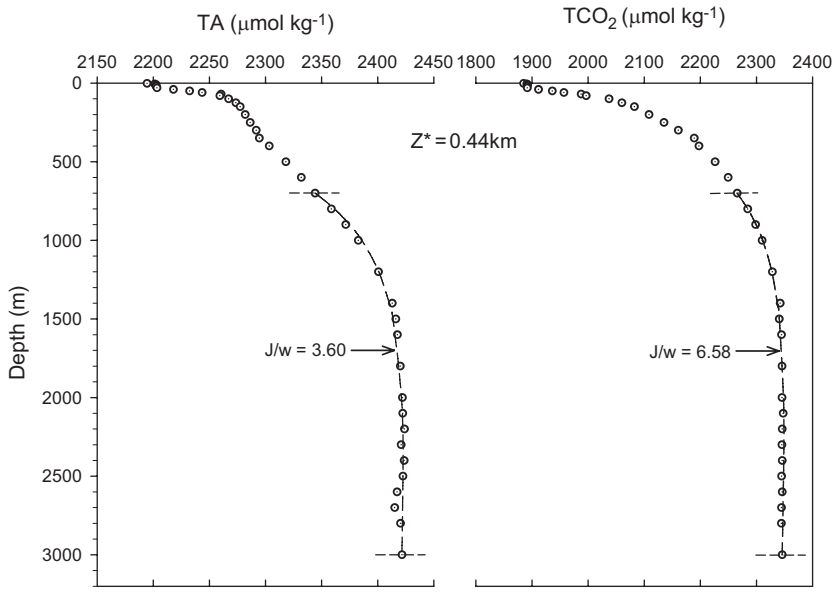

Fig. 8. Measured (A) TCO_2 and (B) TA data with calculated profiles from the diffusion–advection-production model (dashed line) at the SEATS site. The values of Z* and J/w are the best fit values calculated for the deep water between the boundary depths of 700 and 3000 m.

where $\delta^{13}C^{meas}$, $\delta^{13}C^{org'}$, and $\delta^{13}C^{carb'}$ were $\delta^{13}C$ in TCO_2^{meas}, TCO_2^{org} and TCO_2^{carb}, respectively, and values of −20‰ for $\delta^{13}C^{org'}$ (Goericke and Fry, 1994) and +2‰ for $\delta^{13}C^{carb'}$ (Bonneau et al., 1980) were adopted. Rearranging Eq. (9), $\delta^{13}C^{pre}$ was computed with the following equation:

$$\delta^{13}C^{pre}(in‰) = (\delta^{13}C^{meas} \times TCO_2^{meas} + 20 \times TCO_2^{org} - 2 \times TCO_2^{carb})/(TCO_2^{pre}). \quad (10)$$

Results show that $\delta^{13}C^{pre}$ increases progressively from ~0.7‰ at the surface to ~1.2‰ at 500 m, and then remains in a narrow range (1.2 ± 0.05‰) throughout the water column to 3000 m (open squares in Fig. 9). The light $\delta^{13}C^{pre}$ found in the shallow waters echoes the greater influences of anthropogenic CO_2, which has $\delta^{13}C$ value much lighter than that of seawater (−22 to −32‰; Andres et al., 2000). A further examination of effects of anthropogenic CO_2 on the observed $\delta^{13}C$ trend will be presented in later section.

To further assess the net change in $\delta^{13}C_{TCO_2}$ due to addition of TCO_2^{org}, we have assumed a negligible effect of carbonate dissolution. Thus, $\delta^{13}C^{org}$ can be readily calculated by the following mass balance equation:

$$\delta^{13}C^{org} = [(\delta^{13}C^{pre} \times TCO_2^{pre}) + (-20 \times TCO_2^{org})]/(TCO_2^{pre} + TCO_2^{org}) - \delta^{13}C^{pre}. \quad (11)$$

Fig. 9 shows the depth profile of the calculated $\delta^{13}C^{org}$ plus $\delta^{13}C^{pre}$ (open triangles) and $\delta^{13}C^{meas}$ (open circles). As seen, they are nearly equal. In other words, the observed decrease of $\delta^{13}C^{meas}$ with depth results mainly from organic decomposition, while dissolution of carbonates has little effect on the change of $\delta^{13}C_{TCO_2}$.

3.3. The dissolution and saturation state of carbonates at the SEATS site

The degree of carbonate saturation with respect to aragonite and calcite, i.e. $\Omega_{aragonite}$ and $\Omega_{calcite}$ ($\Omega = [Ca^{2+}] \times [CO_3^{2-}]/Ksp$), was estimated using the program developed by Lewis and Wallace (1998). As shown in Fig. 10, both $\Omega_{aragonite}$ (open triangles) and $\Omega_{calcite}$ (open circles) decrease rapidly with depth in the upper 1000 m due to the decrease of $[CO_3^{2-}]$ (open diamonds). As indicated by open diamonds in Fig. 10, $[CO_3^{2-}]$ decreases dramatically from a surface value of ~220 to ~70 μmol kg^{-1} at 1000 m, and this drop can account for ~80% of the decrease of saturation in the upper 1000 m. By contrast, $[CO_3^{2-}]$ stays relatively constant below 1000 m. As a consequence, the continuous decrease in saturation must have resulted from the increase of Ksp due to the increase of pressure and decrease of temperature with depth. As revealed in Fig. 10, the saturation depths of aragonite and calcite could be placed at about 600 and 2500 m, respectively, at the SEATS site. The calculated depths derived from this study are consistent with those reported in the same latitude of NWP by Feely et al. (2002) (Table 1).

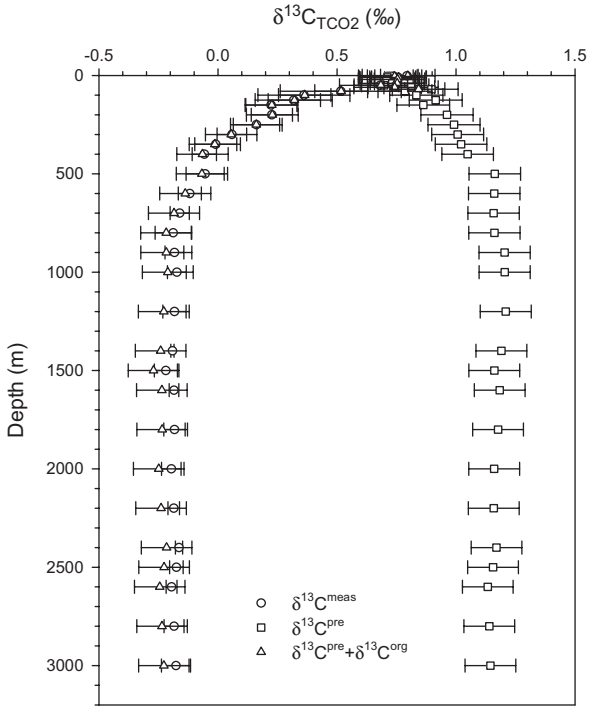

Fig. 9. Depth profiles of measured $\delta^{13}C$ ($\delta^{13}C^{meas}$), preformed $\delta^{13}C$ ($\delta^{13}C^{pre}$), and $\delta^{13}C^{pre} + \delta^{13}C^{org}$ at the SEATS site. See details in text for the definition and calculation of $\delta^{13}C^{org}$. Open circle and horizontal bar represent the average and variation of $\delta^{13}C^{meas}$ at a given depth from the eight cruises between March 2002 and October 2003. Horizontal bars on $\delta^{13}C^{pre}$ and $\delta^{13}C^{pre} + \delta^{13}C^{org}$ profiles represent the uncertainties in their calculations.

To assess further the depth levels where carbonate dissolution actually took place in water column at the SEATS site, we superimposed the depth distribution of TCO_2^{carb} (TCO_2 produced by carbonate dissolution; termed as TA* by Feely et al. (2002) and Sabine et al. (2002b), and as ΔTA^{CaCO_3} by Chung et al. (2003) on $\Omega_{aragonite}$ and $\Omega_{calcite}$ depth profiles in Fig. 10 (open squares). It is found that appreciable TCO_2^{carb} is present in waters well above the calcite saturation depth (~2500 m), even at depths shallower than the aragonite saturation depth (~600 m). Thus, TCO_2^{carb} data indicate that carbonate dissolution might take place at depths shallower than those assessed by saturation data. Although the consensus has been that shallow waters are supersaturated with respect to both aragonite and calcite, and appreciable carbonate dissolution only occurs at greater depths in the ocean, recent studies have suggested that dissolution of carbonates might occur in shallow waters. For instance, Milliman et al. (1999) reported that as much as 60–80% of carbonates exported from the surface layer have been remineralized in the upper 500–1000 m of the ocean. Feely et al. (2002), Sabine et al. (2002b), and Chung et al. (2003) found that excess TA did exist in the shallow water at depths well above the calcite lysocline in the Pacific, the Indian, and the Atlantic oceans. Our results thus are in consistent with their conclusion. Nevertheless, it should be pointed out that our estimates from excess TA data represent the uppermost limit of

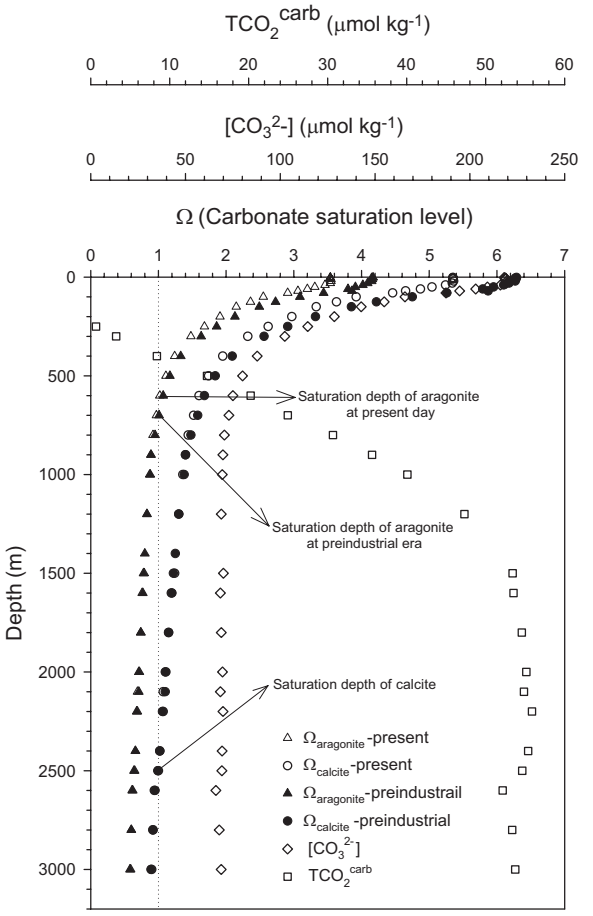

Fig. 10. Depth profiles of aragonite ($\Omega_{aragonite}$) and calcite ($\Omega_{calcite}$) saturation levels at the present time (open triangles and circles) and the pre-industrial era (solid triangles and circles) at the SEATS site. Superimposed are the depth profiles of concentration of carbonate ion ($[CO_3^{2-}]$, open diamonds) and TCO_2^{carb} (TCO_2 produced from carbonate dissolution, open squares).

dissolution because the upwards advection of TA-enriched deep water, the sedimentary calcite dissolution in the sediment–water interface (de Villiers, 2005) and the denitrification and reduction of organic matter by manganese, iron, and sulfate in the anaerobic environment on the shelves (Chen, 2002) also could contribute to the excess TA found in shallow waters. In fact, there have been various possible mechanisms proposed to explain the carbonate dissolution at the shallower depths, e.g. (1) dissolution within the guts and feces of zooplankton (Jansen and Ahrens, 2004; and references therein); (2) the microbial oxidation of organic matter may produce a microenvironment conducive to carbonate dissolution (Milliman et al., 1999); (3) dissolution of more soluble carbonate phases, such as pteropods and high-magnesium calcite (Feely et al., 2002). Consequently, the appearance of excess TA in shallow waters is suggested to multiple interpretations and required further investigation.

3.4. The penetration of anthropogenic CO_2 and its influence on the saturation state of carbonate

Observation-based methods for estimating the penetration and storage of anthropogenic CO_2 in the ocean are derived either from the carbon chemistry (mainly TA and TCO_2) or the $\delta^{13}C$ data (Wallace, 2001; Quay et al., 2003). In this study, we utilized these two data sets separately, which were measured concurrently, to assess the magnitude of anthropogenic CO_2 (excess CO_2) influence in the water column at the SEATS site.

The back calculation method of Chen and Millero (1979) was adopted to estimate the influence of anthropogenic CO_2 on TCO_2 in the water column. The underlying principle of this method and some alterations have been described in great detail by Chen and Millero (1979), Chen and Pytkowicz (1979), Gruber et al. (1996), Sabine and Feely (2001), and Wallace (2001). In this study, changes in $NTCO_2$ resulted from remineralization of organic carbon and carbonate dissolution were estimated by Eqs. (6) and (7), respectively. The preformed TA at the present time was calculated by Eq. (4). The preformed $NTCO_2$ at the present time ($NTCO_{2\ present}^{pre}$) was calculated separately using the following equations (Chen et al., 1986; Chen and Huang, 1995):

For the DW:

$$NTCO_{2\ present}^{pre}(\mu mol\,kg^{-1}) = 2219 - 11 \times \theta(\pm 16). \quad (12)$$

For waters above and the $S_{min}W$:

$$NTCO_{2\ present}^{pre}(\mu mol\,kg^{-1}) = 2242 - 12.08 \times \theta(\pm 18). \quad (13)$$

At depth where the $S_{min}W$ mixed with DW, the θ/S plot was further used to estimate their respective contribution. For surface waters, the "anthropogenic CO_2" was estimated from the difference between measured $NTCO_2$ and the "preindustrial $NTCO_2$", which was computed from the measured TA and hydrographical data assuming that pCO_2 of seawater was at equilibrium with atmospheric pCO_2

of 280 ppmv. Although there were considerable uncertainties ($\pm 20\,\mu mol\,kg^{-1}$) associated with this method (Shiller, 1981; Chen et al., 1982), it is thus far the only approach applicable for a single site's assessment such as the SEATS.

Results from these calculations are depicted in Fig. 11. As shown, concentrations of anthropogenic CO_2 decrease exponentially with depth. Below 1000 m, they fluctuate slightly around $0 \pm 5\,\mu mol\,kg^{-1}$, implying the maximal depth they could reach. The penetration depth at ~1000 m is in good agreement with other studies reported previously in the North Pacific (Chen, 1987; Sabine et al., 2002a; Table 1). Nonetheless, the concentration of anthropogenic CO_2 in the surface water (~between 55 and $60\,\mu mol\,kg^{-1}$) is appreciably higher than that reported by Sabine et al. (2002a) in subtropical surface water of the North Pacific Ocean (between 40 and $50\,\mu mol\,kg^{-1}$). The discrepancy is attributed to the different sampling time between that of Sabine et al. (2002a) and ours (1991–1994 vs. 1999–2003) because more anthropogenic CO_2 must have accumulated in surface waters at the SEATS site. The total column inventory of anthropogenic CO_2 was estimated to be $\sim 16.6\,mol\,m^{-2}$ at the SEATS site, which was slightly less than $\sim 20\,mol\,m^{-2}$ reported by Sabine et al. (2002a) for the same latitude in the NWP (Table 1). The difference can be best explained by the greater upward advection (upwelling) in the SCS that tends to reduce its capacity in storing both natural and anthropogenic CO_2. By extrapolating this value to the entire SCS ($3.5 \times 10^6\,km^2$), the total anthropogenic CO_2 in the SCS is about 0.5 ± 0.2 PgC (1 PgC = 10^{15} g carbon), i.e. 0.42% of total anthropogenic CO_2 storage in the global oceans (118 ± 19 PgC; Sabine et al., 2004). The value is rather small, considering the SCS's share in terms of size that occupies 0.97% of the total ocean. It thus appears that, unlike other marginal seas in high latitude such as the Bering Sea and the Sea of Okhotsk, SCS plays only a minor role in transporting anthropogenic CO_2 to the interior of the North Pacific.

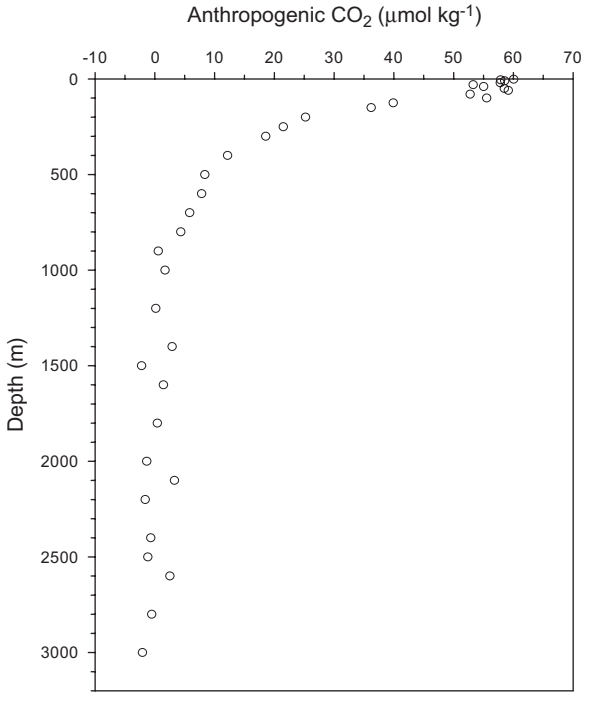

Fig. 11. Depth profile of anthropogenic CO_2 at the SEATS site.

To assess further aragonite and calcite saturation states of seawaters in the preindustrial era, we assumed that TA did not change during industrial era, and the preindustrial levels of TCO_2 could be calculated by subtracting the anthropogenic CO_2 concentration from the TCO_2 measured. Results show that the depth of calcite saturation during preindustrial era is same as that of the present day, while the depth of aragonite saturation has migrated upward approximately 100 m. The upward migration of aragonite saturation depth implies that carbonate particles settling through the water column may dissolve at shallower depths and decrease the supply of sinking particles to bottom sediments in the SCS during industrial era. The saturation levels of aragonite and calcite in surface waters have decreased considerably from the preindustrial values of ~4.2 and ~6.3 to ~3.5 and ~5.4 at present, respectively, due to the uptake of anthropogenic CO_2. Recently Feely et al. (2004) reported that the calcification rate of all calcifying organisms had decreased in response to a lowered carbonate saturation state, even when the carbonate saturation level was >1. The decrease of carbonate saturation found in the SCS is in line with their observations and deserved to be further investigated.

Conventionally, estimates of anthropogenic CO_2 penetration from $\delta^{13}C$ data could be furnished directly by temporal changes in $\delta^{13}C$ (Quay et al., 2003, and references therein) or indirectly by the concurrent $\delta^{13}C$-nutrient method (Keir et al., 1998; Ortiz et al., 2000). We had adopted the latter to assess the influence of anthropogenic CO_2 on $\delta^{13}C$ in this study because of the lack of historical

measurements of $\delta^{13}C$ at SEATS site. As discussed in Section 3.2.3, vertical distribution of $\delta^{13}C$ is primarily controlled by the biological cycling of ^{13}C-depleted organic matter in the water column, and thus a negative correlation between $\delta^{13}C$ and nutrients should exist. According to Broecker and Maier-Reimer (1992), the slope in the plot of $\delta^{13}C$ vs. phosphate should be about −1.1, providing that there was no isotopic exchange between seawaters and the overlying atmosphere. The correlation between $\delta^{13}C$ and phosphate at the SEATS site is plotted in Fig. 12. As seen, the slopes of correlation are much less negative (−0.71 and −0.23 for waters above and below 100 m, respectively) than the expected biological trend (−1.1). Lin et al. (1999) reported a similar deviation in the northeastern SCS. These deviations imply that processes other than biological cycling, such as isotopic fractionations and uptake of anthropogenic CO_2 during air–sea CO_2 exchange, must have been involved in decoupling the expected correlation between $\delta^{13}C$ and phosphate (Lynch-Stieglitz et al., 1995).

The influence of the air–sea exchange on oceanic $\delta^{13}C$ consists of three components, i.e. thermodynamic, kinetic, and anthropogenic CO_2 effects (Keir et al., 1998; Ortiz et al., 2000). According to Zhang et al. (1995), the temperature-dependent isotopic fractionation of $\delta^{13}C$ associated with the air–sea equilibration is about −0.1‰ $^{\circ}K^{-1}$. As a result, a thermodynamic effect tends to make $\delta^{13}C$ in cold surface water higher than that in warm surface water. The kinetic effects cause surface waters to be enriched in ^{13}C in source areas, and depleted in sink areas (Lynch-Stieglitz et al., 1995). According to Broecker and Maier-Reimer (1992), the net effect of the air–sea exchange on the surface ocean $\delta^{13}C$ can be derived from the following relationship:

$$\delta^{13}C_{as} = \delta^{13}C^{meas} - (2.7 - 1.1 \times [PO_4^{3-}]), \qquad (14)$$

where $\delta^{13}C_{as}$ stands for $\delta^{13}C$ that is affected by the air–sea exchange. The term in parenthesis on the right-hand side of Eq. (14) is the mean ocean biological trend. Fig. 12 shows the $\delta^{13}C_{as}$ (the offset between $\delta^{13}C^{meas}$ and the hypothetical mean ocean biological trend) is negative for waters shallower than ~800 m (phosphate < 2.6 μmol kg^{-1}), while it is slightly positive for waters below. The negative $\delta^{13}C_{as}$ in shallow waters, however, cannot be attributed to thermodynamic and kinetic effects alone, i.e. deriving from a high temperature and/or a sink area. Instead, portions of the negative $\delta^{13}C_{as}$ signal must have come from the anthropogenic CO_2, which is depleted in ^{13}C and penetrates to a depth of ~1000 m as discussed previously. For deep waters, positive $\delta^{13}C_{as}$ indicates that the waters originate from a low temperature and/or source area.

According to Keir et al. (1998) and Ortiz et al. (2000), the combined thermodynamic and kinetic effect, and anthropogenic CO_2 effect on $\delta^{13}C_{as}$ can be resolved from establishing a pre-anthropogenic relation model between $\delta^{13}C$ and phosphate in the study area. The offset between pre-anthropogenic model and $\delta^{13}C^{meas}$, denoted as $\Delta\delta^{13}C_{a-p}$, represented the magnitude of the anthropogenic CO_2 on $\delta^{13}C_{as}$, while the offset between mean ocean biological trend and pre-anthropogenic model, denoted as $\Delta\delta^{13}C_{ther}$, signified the combined thermodynamic and kinetic effects on $\delta^{13}C_{as}$ (Fig. 12). Here, we employed the similar technique of Keir et al. (1998) and Ortiz et al. (2000) with minor modifications to establish the pre-anthropogenic model for the SEATS site. We first assumed that waters below 2000 m contained no anthropogenic CO_2, because deep waters in the SCS originate from the NPDW, the oldest water mass in the global oceans, so that they had exchanged with the atmosphere before the presence of anthropogenic CO_2. We further assumed that the surface water $\delta^{13}C$ has decreased by 1.0‰ since the

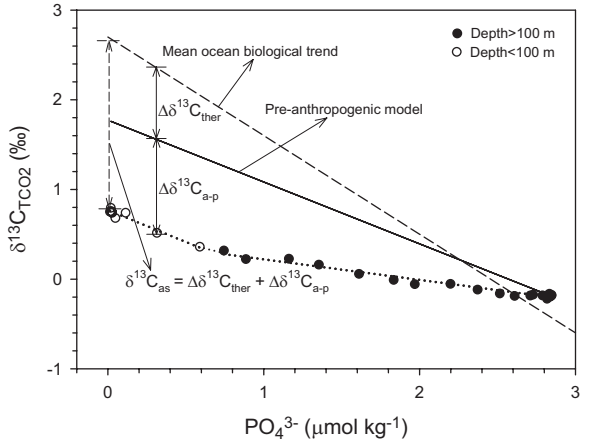

Fig. 12. The correlation between $\delta^{13}C_{TCO_2}$ and phosphate at the SEATS site. The dashed and solid lines denote respectively the hypothetical mean ocean biological trend and that derived from the pre-anthropogenic model. In addition, superimposed are two regression lines (dotted) calculated separately from water samples above (open circles) and below (solid circles) 100 m. See details in text for the definitions and calculations of the mean ocean biological trend, the pre-anthropogenic model, $\delta^{13}C_{as}$, $\Delta\delta^{13}C_{ther}$, and $\Delta\delta^{13}C_{a-p}$.

pre-anthropogenic era. This assumption was made because $\delta^{13}C$ in the surface ocean waters had decreased by about 0.8‰ from the last 200 years to the end of 1992 (Böhm et al., 1996) and a rate of $\delta^{13}C$ decrease during the past decade in the surface water of the North Pacific was approximately 0.2‰ (Sonnerup et al., 1999). By connecting the surface and deep end-points, the pre-anthropogenic model at SEATS was established (solid line in Fig. 12), and then the magnitude of anthropogenic CO_2 influence on $\delta^{13}C$ ($\Delta\delta^{13}C_{a-p}$) can be estimated by the offset between the established pre-anthropogenic model and $\delta^{13}C^{meas}$.

The depth distribution of $\Delta\delta^{13}C_{a-p}$ is depicted on Fig. 13. As seen in Fig. 11, the vertical variations of $\Delta\delta^{13}C_{a-p}$ (derived from isotopic data) are very similar to those of "anthropogenic CO_2" (derived from TA and TCO_2 data). Both approaches indicate that the influence of anthropogenic CO_2 has penetrated to approximately 1000 m in the water column. Furthermore, an averaged $\Delta\delta^{13}C/\Delta TCO_2$ ratio of -0.026‰ $(\mu mol\,kg^{-1})^{-1}$ throughout the penetration depth was obtained by dividing the depth-integrated $\Delta\delta^{13}C_{a-p}$ (~ -426‰ m) with the depth-integrated "anthropogenic CO_2" ($\sim$16,600 $\mu mol\,kg^{-1}$ m). This value is almost identical to the $\Delta\delta^{13}C/\Delta TCO_2$ ratio (-0.024‰ $(\mu mol\,kg^{-1})^{-1}$) estimated from the temporal changes of TCO_2 and $\delta^{13}C$ at HOT (Winn et al., 1998; Gruber et al., 1999; Table 1) and the North Atlantic Ocean (Körtzinger et al., 2003). It differs, however, from ratios between -0.007 and -0.015‰ $(\mu mol\,kg^{-1})^{-1}$ in the Southern Ocean (McNeill et al., 2001), -0.013‰ $(\mu mol\,kg^{-1})^{-1}$ in the southern Indian Ocean (Chen and Chen, 1989), and -0.016‰ $(\mu mol\,kg^{-1})^{-1}$ in the northeastern Atlantic (Keir et al., 1998).

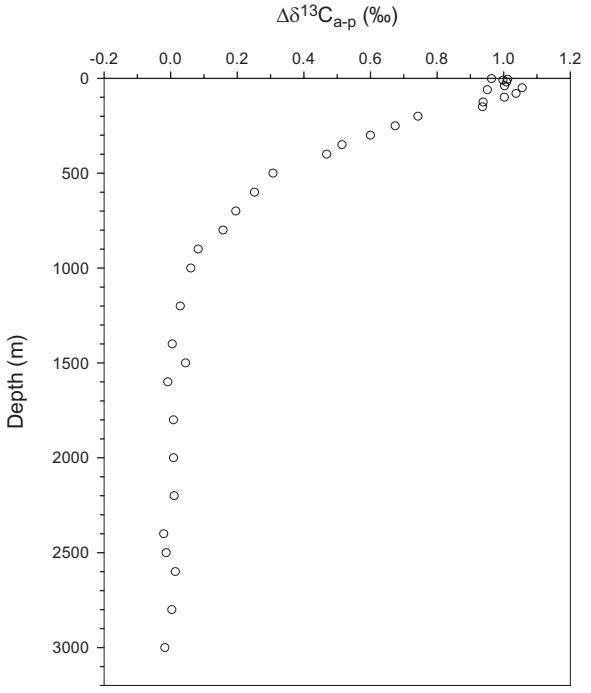

Fig. 13. Depth profile of $\Delta\delta^{13}C_{a-p}$ at the SEATS site. See text for the definition and calculation of "$\Delta\delta^{13}C_{a-p}$" in details.

4. Conclusions

In this study, we thoroughly investigated the vertical distributions of TA, TCO_2 and $\delta^{13}C_{TCO_2}$ in the water column at SEATS site, northern SCS, which were collected from 19 different cruises spanning from September 1999 to October 2003. The depth profiles were then compiled to document their general distributions in the SCS. Furthermore, in order to understand better processes controlling their variations and to better quantify the influence of the anthropogenic CO_2 upon their distributions, we have deconvoluted these profiles into different components using various techniques that were widely used in marine biogeochemical community. The effort thus ensured our results to be comparable with data from other studies, and to be used in the future for a better coverage of carbon synthesis in the world oceans.

The property vs. salinity plots revealed that depth distributions of TA, TCO_2 and $\delta^{13}C_{TCO_2}$ in the water column at SEATS were affected chiefly by the water mass structure and the rapid vertical advection in the SCS. The vertical gradients of these parameters were all controlled, to different extent, by production/decomposition of organic matter, formation/dissolution of carbonates, and differences in their respective preformed values. For NTA, due to the compensation of increment in preformed values and consumption of TA during organic decomposition, it remained nearly constant in the top 150 m of water column. From 150 to 350 m, the increase of NTA results principally from the increase in preformed values, whereas carbonate dissolution accounted for the continuous rise in NTA below 350 m. For $NTCO_2$, increases in preformed values and organic oxidation with depth were equally important in controlling the observed increasing trend in the upper 400 m. Below 400 m, although carbonate dissolution together with organic decomposition and increase of preformed

values led to the continuous increase of $NTCO_2$ with depth, carbonate dissolution had a minor effect. As shown by results from stoichiometric model and the one dimensional diffusion-advection model, carbonate dissolution contributed to ~25% of added TCO_2. The decrease of $\delta^{13}C_{TCO_2}$ with depth, however, was attributed mainly to organic oxidation throughout the water column. Moreover, calculations of saturation level of carbonates showed that the saturation level of aragonite and calcite decreased 17% and 14%, respectively, in the surface water, and the aragonite saturation depth had migrated upward ~100 m since the industrial revolution. Nonetheless, the observed TA^{carb} emerged at depths shallower than those hypothetically estimated from calcite and aragonite saturations, may also result from the biologically mediated dissolution of carbonate, upwards advection of TA-enriched deep water, and TA generated by anaerobic reduction reactions in shelves' sediments.

The depth of anthropogenic CO_2 penetration in the water column at the SEATS site was estimated using two independent indicators, namely "anthropogenic CO_2" and "$\Delta\delta^{13}C_{a-p}$", which were derived from the "back calculation" and "$\delta^{13}C$ vs. phosphate" methods, respectively. Results show that anthropogenic CO_2 has penetrated to a depth of ~1000 m. The calculated column inventory of anthropogenic CO_2 is slightly less than that in the same latitude of the NWP (~16.6 vs. ~20 mol m^{-1}), suggesting a greater upward advection in the SCS. Since more anthropogenic CO_2 invasion is anticipated, results from this study could provide a baseline for future studies of the impacts of anthropogenic CO_2 on the carbon system in the SCS.

Acknowledgments

We are grateful to the Captains, crew and technicians of *R/V Ocean Research I* and *III* for assistance with deck operations and shipboard sampling, and to C.N. Sun, S.L. Lee, and Y.Y. Shih for laboratory assistance. We appreciate K.K. Liu, L.S. Wen, F.K. Shiah, and staff of the National Center for Ocean Research (NCOR) for cruise participation and logistic supports during the course of this research. Constructive comments and suggestions from two anonymous reviewers have greatly improved the manuscript. This work was supported by the National Science Council grants (NSC90-2611-M-110-025-OP1, NSC91-2611-M-110-003 and NSC92-2119-M-110-001) to D.D. Sheu. The study is a contribution (#107) to the SEATS program sponsored by NCOR, National Science Council, Republic of China.

References

Anderson, L.A., Sarmiento, J.L., 1994. Redfield ratios of remineralization determined by nutrient data analysis. Global Biogeochemical Cycles 8, 65–80.

Andres, R.J., Marland, G., Boden, T., Bischoff, S., 2000. Carbon dioxide emissions from fossil fuel consumption and cement manufacture, 1751 to 1991, and an estimate of their isotopic composition and latitudinal distribution. In: Wigley, T.M.L., Schimel, S. (Eds.), The Carbon Cycle. Cambridge University Press, New York, pp. 53–62.

Böhm, F., Joachimski, M.M., Lehnert, H., Morgenroth, G., Kretschmer, W., Vacelet, J., Dullo, W.C., 1996. Carbon isotope records from extant Caribbean and South Pacific sponges: evolution of $\delta^{13}C$ in surface water DIC. Earth Planetary Science Letters 139, 291–303.

Bonneau, M.C., Bergnaud-Grazzini, C., Berger, W.H., 1980. Stable isotope fractionation and differential dissolution in recent planktonic foraminifera from Pacifc box cores. Oceanologica Acta 3, 377–382.

Broecker, W.S., Maier-Reimer, E., 1992. The influence of air and sea exchange on the carbon isotope distribution in the sea. Global Biogeochemical Cycles 6, 315–320.

Butler, J.N., 1992. Alkalinity titration in seawater: how accurately can the data be fitted by an equilibrium model? Marine Chemistry 38, 251–282.

Chao, S.Y., Shaw, P.T., Wu, S.Y., 1996. Deep water ventilation in the South China Sea. Deep-Sea Research I 43, 445–466.

Chen, C.T.A., 1987. On the depth of anthropogenic CO_2 penetration in the Atlantic and Pacific Oceans. Oceanologica Acta, 97–102.

Chen, C.T.A., 1990. Rates of calcium carbonate dissolution and organic carbon decomposition in the North Pacific Ocean. Journal of the Oceanography Society of Japan 46, 201–210.

Chen, C.T.A., 2002. Shelf-vs. dissolution-generated alkalinity above the chemical lysocline. Deep-Sea Research II 49, 5365–5375.

Chen, C.T.A., Huang, M.H., 1995. Carbonate chemistry and the anthropogenic CO_2 in the South China Sea. Acta Oceanologica Sinica 14, 47–57.

Chen, C.T.A., Millero, F.J., 1979. Gradual increase of oceanic CO_2. Nature 277, 205–206.

Chen, C.T.A., Pytkowicz, R.M., 1979. On the total CO_2-titration alkalinity-oxygen system in the Pacific Ocean. Nature 281, 362–365.

Chen, C.T.A., Millero, F.J., Pytkowicz, R.M., 1982. Comment on calculating the oceanic CO_2 increase: a need for caution by A. M. Shiller. Journal of Geophysical Research 87, 2083–2085.

Chen, C.T.A., Rodmam, M.R., Wei, C.L., Olson, E.J., Feely, R.A., 1986. Carbonate Chemistry of the North Pacific Ocean. US Department of Energy Technical Report, DOE/NBB-0079, p. 176.

Chen, C.T.A., Wang, S.L., Chou, W.C., Sheu, D.D., 2006. Carbonate chemistry and projected future changes in pH and

$CaCO_3$ saturation state of the South China Sea. Marine Chemistry 101, 277–305.

Chen, D.W., Chen, C.T.A., 1989. The anthropogenic CO_2 signals in the Indian Ocean. Journal of the Environmental Protection Society of the Republic of China 12, 46–65 (in Chinese with English abstract).

Chou, W.C., Sheu, D.D., Chen, C.T.A., Wang, S.L., Tseng, C.M., 2005. Seasonal variability of carbon chemistry at the SEATS time-series site, northern South China Sea between 2002 and 2003. Terrestrial Atmospheric and Oceanic Sciences 16, 445–465.

Chou, W.C., Chen, Y.L.L., Sheu, D.D., Shih, Y.Y., Han, C.A., Cho, C.L., Yang, Y.J., Tseng, C.M., 2006. Estimated net community production during the summer season at the SEATS site: implications for nitrogen fixation. Geophysical Research Letters 33, L22610.

Chung, S.N., Lee, K., Feely, R.A., Sabine, C.L., Millero, F.J., Wanninkhof, J.L., Bullister, Key, R.M., Peng, T.H., 2003. Calcium carbonate budget in the Atlantic Ocean based on water column inorganic carbon chemistry. Global Biogeochemical Cycles 17.

Chung, Y.C., Craig, H., 1973. Radium-226 in the eastern equatorial Pacific. Earth and Planetary Science Letters 17, 306–318.

Craig, H., 1957. Isotopic standards for carbon and oxygen and correction factors for mass-spectrometric analysis of carbon dioxide. Geochimica et Cosmochimica Acta 12, 133–149.

Craig, H., 1969. Abyssal carbon and radiocarbon in the Pacific. Journal of Geophysical Research 74, 5491–5506.

Craig, H., Weiss, R.F., 1970. The Geosecs 1969 intercalibration station: introduction, hydrographic features, and total CO_2–O_2 relationships. Journal of Geophysical Research 75, 7641–7647.

de Villiers, S., 2005. Foraminiferal shell-weight evidence for sedimentary calcite dissolution above the lysocline. Deep-Sea Research I 52, 671–680.

DOE, 1994. Handbook of methods for the analysis of the various parameters of the carbon dioxide system in seawater. In: Dickson, A.G., Goyet, C., (Eds.), US Department of Energy CO_2 science Team Report, version 2 (unpublished manuscript).

Gong, G.C., Liu, K.K., Liu, C.T., Pai, S.C., 1992. The chemical hydrography of the South China Sea west of Luzon and a comparison with the West Philippine Sea. Terrestrial Atmospheric and Oceanic Science 3, 587–602.

Feely, R.A., Sabine, C.L., Lee, K., Millero, F.L., Lamb, M.F., Greeley, D., Bullister, J.L., Key, R.M., Peng, T.H., Kozyr, A., Ono, T., Wong, C.S., 2002. In situ calcium carbonate dissolution in the Pacific Ocean, global biogeochemical cycles 16.

Feely, R.A., Sabine, C.L., Lee, K., Berelson, W., Kleypas, J., Fabry, V.J., Millero, F.J., 2004. Impact of anthropogenic CO_2 on the $CaCO_3$ system in the oceans. Science 305, 362–366.

Goericke, R., Fry, B., 1994. Variations of marine plankton $\delta^{13}C$ with latitude, temperature, and dissolved CO_2 in the world ocean. Global Biogeochemical Cycles 8, 85–90.

Gruber, N., Sarmiento, J.L., Stocker, T.F., 1996. An improved method for detecting anthropogenic CO_2 in the oceans. Global Biogeochemical Cycles 10, 809–837.

Gruber, N., Keeling, C.D., Bacastow, R.B., Guenther, P.R., Lueker, T.J., Wahlen, M., Meijer, H.A.J., Mook, W.G., Stocker, T.F., 1999. Spatiotemporal patterns of carbon-13 in the global surface oceans and the oceanic Suess effect. Global Biogeochemical Cycles 13, 307–335.

Jansen, H., Ahrens, M.J., 2004. Carbon dissolution in the guts of benthic deposit feeders: a numerical model. Geochimica et Cosmochimica Acta 68, 4077–4092.

Keir, R., Rehder, G., Suess, E., 1998. The $\delta^{13}C$ anomaly in the Northeastern Atlantic. Global Biogeochemical Cycles 12, 467–477.

Körtzinger, A., Quay, P.D., Sonnerup, R.E., 2003. Relationship between anthropogenic CO_2 and ^{13}C Suess effect in the North Atlantic Ocean. Global Biogeochemical Cycles 17.

Kroopnick, P.M., 1985. The distribution of ^{13}C of TCO_2 in the world oceans. Deep-Sea Research 32, 57–84.

Lewis, E.D., Wallace, W.R., 1998. Program developed for CO_2 system calculations. Report 105, Oak Ridge National. Laboratory, US Department of Energy, Oak Ridge, Tenn.

Lin, H.L., Wang, L.W., Wang, C.H., Gong, G.C., 1999. Vertical distribution of $\delta^{13}C$ of dissolved inorganic carbon in Northeastern South China Sea. Deep-Sea Research I 46, 757–775.

Lynch-Stieglitz, J., Stocker, T.F., Broecker, W.S., Fairbanks, R.G., 1995. The influence of air-sea exchanges on the isotopic composition of oceanic carbon: observations and modeling. Global Biogeochemical Cycles 9, 653–666.

McNeill, B.I., Matear, R.J., Tilbrook, B., 2001. Does carbon 13 track anthropogenic CO_2 in the Southern Ocean? Global Biogeochemical Cycles 15, 597–614.

Milliman, J.D., Troy, P.J., Balch, W.M., Adams, A.K., Li, Y.H., Mackenzie, F.T., 1999. Biological mediated dissolution of calcium carbonate above the chemical lysocline. Deep-Sea Research I 46, 1653–1669.

Nitani, H., 1972. Beginning of the Kuroshio. In: Stommel, H., Yoshida, K., (Eds.), University of Washington Press, Washington, pp. 129–163.

Ortiz, J.D., Mix, A.C., Wheeler, P.A., Key, R.M., 2000. Anthropogenic CO_2 invasion into the northeast Pacific based on concurrent $\delta^{13}C_{DIC}$ and nutrient profiles from the California Current. Global Biogeochemical Cycles 14, 917–929.

Quay, P., Sonnerup, R., Westby, T., Stutsman, J., McNichol, A., 2003. Changes in the $^{13}C/^{12}C$ of dissolved inorganic carbon in the ocean as a tracer of anthropogenic CO_2 uptake. Global Biogeochemical Cycles 17.

Sabine, C.L., Feely, R.A., 2001. Comparison of recent Indian Ocean anthropogenic CO_2 estimates with a historical approach. Global Biogeochemical Cycles 15, 31–42.

Sabine, C.L., Feely, R.A., Key, R.M., Bullister, J.L., Millero, F.L., Lee, K., Peng, T.H., Tilbrook, B., Wong, C.S., 2002a. Distribution of anthropogenic CO_2 in the Pacific Ocean. Global Biogeochemical Cycles 16.

Sabine, C.L., Key, R.M., Feely, R.A., Greeley, D., 2002b. Inorganic carbon in the Indian Ocean: distribution and dissolution processes. Global Biogeochemical Cycles 16.

Sabine, C.L., Feely, R.A., Gruber, N., Key, R.M., Lee, K., Bullister, J.L., Wannikhof, R., Wong, C.S., Wallace, D.W.R., Tilbrook, B., Millero, F.J., Peng, T.H., Kozyr, A., Ono, T., Rios, A.F., 2004. The oceanic sink for anthropogenic CO_2. Science 305, 367–371.

Shaw, P.T., Chao, S.Y., Liu, K.K., Pai, S.C., Liu, C.T., 1996. Winter upwelling off Luzon in the northeastern South China Sea. Journal of Geophysical Research 101, 16435–16448.

Sheu, D.D., Lee, W.Y., Wang, C.H., Wei, C.L., Chen, C.T.A., Cherng, C., Huang, M.H., 1996. Depth distribution of $\delta^{13}C$ of

dissolved ΣCO_2 in seawater off eastern Taiwan: effects of the Kuroshio current and its associated upwelling phenomenon. Continental Shelf Research 16, 1609–1619.

Shiller, A.M., 1981. Calculating the oceanic CO_2 increase: a need for caution. Journal of Geophysical Research 86, 11083–11088.

Sonnerup, R.E., Quay, P.D., McNichol, A.P., Bullister, J.L., Westby, T.A., Anderson, H.L., 1999. Reconstructing the oceanic ^{13}C Suess effect. Global Biogeochemical Cycles 13, 857–872.

Thomas, H., Bozec, Y., Elkalay, K., de Baar, H.J.W., 2004. Enhanced open ocean storage of CO_2 from shelf sea pumping. Science 304, 1005–1008.

Tseng, C.M., Wong, G.T.F., Chou, W.C., Lee, B.S., Sheu, D.D., Liu, K.K., 2007. Temporal variations in the carbonate system in the upper layer at the SEATS station. Deep-Sea Research II, this issue [doi:10.1016/j.dsr2.2007.05.003].

Wallace, D.W.R., 2001. Introduction to special section: ocean measurements and models of carbon sources and sinks. Global Biogeochemical Cycles 15, 3–10.

Winn, C.D., Li, Y.H., Mackenzie, F.T., Karl, D.M., 1998. Rising surface ocean dissolved inorganic carbon at the Hawaii Ocean Time-series site. Marine Chemistry 60, 33–47.

Zhang, J., Quay, P.D., Wilbur, D.O., 1995. Carbon isotope fractionation during gas–water exchange and dissolution of CO_2. Geochimica et Cosmochimica Acta 59, 107–114.